JOURNAL OF GEOPHYSICAL RESEARCH, VOL. 97, NO. A3, PAGES 2935–2942, MARCH 1, 1992

Observation of Dust Shedding From Material Bodies in a Plasma

T. E. SHERIDAN[1] AND J. GOREE[2]

Department of Physics and Astronomy, University of Iowa, Iowa City

Y. T. CHIU, R. L. RAIRDEN, AND J. A. KIESSLING

Lockheed Palo Alto Research Laboratory, Palo Alto, California

Exposure to a space plasma can cause a dusty body, such as a spacecraft or a boulder in Saturn's rings, to release dust into its environment. This is demonstrated in a laboratory experiment with an aluminum sphere covered with micrometer-sized dust grains. The sphere was rotating and electrically floating like an object in space. Laser light scattering was used to detect dust falling from the body. When a low-temperature nitrogen plasma was turned on, rapid dust shedding was observed, and when it was turned off, the shedding stopped. The rate of shedding increases with plasma density. The dust is not all released the instant the plasma is turned on but rather takes place over an extended period of time, with individual grains jumping off at random intervals with a certain probability per unit time.

1. INTRODUCTION

Plasma dust interactions have been recognized to be of cosmic significance for some years [*Goertz*, 1989, and references therein]. By dust we mean macroscopic particles with a typical size of a micrometer. These particles are vastly more massive than a single ion but have a characteristic size much less than the Debye length. In the near-Earth space environment, micrometer-sized particulates are responsible for the micrometeoroid belts and noctilucent clouds in the upper atmosphere, for example. Other dusty plasmas include planetary rings and presolar nebulae. What makes a plasma different when it is dusty is that dust grains become electrically charged. They act somewhat like very heavy ions and deplete the electron density.

In this paper we introduce a new variety of plasma-dust experiments by including a large dusty object in the plasma. By large we mean much wider than a Debye length. This topic is relevant to questions as diverse as the formation of spokes in the Saturnian ring system and dust shedding by spacecraft. The question that we ask here is how can the dust be released from the surface of a large object. A few authors have already investigated the complementary question of what might happen after the dust has been released.

Murphy and Chiu [1991] reported computer simulations of a spacecraft surrounded by a dust cloud. Such a dust cloud can be a problem in spacecraft operation when it leads to unwanted light scattering in front of a telescope or an optical tracker. Murphy and Chiu assumed a spherical body immersed in a plasma with a low dust density and Maxwellian velocity distributions. Their dynamic simulation, with boundary conditions imposed by the spacecraft, revealed that the charge on the body was diminished because of the presence of the dust and also that the density of the dust cloud was reduced by the presence of the body.

Geophysical researchers have noted that the ring systems in the magnetospheres of the outer planets contain both dust grains and large (i.e., large in comparison with to the Debye length) dust-covered boulders. For example, *Shan* [1990] modeled the release of dust from boulders in Saturn's ring system. He found that the short-lived, dense ($n_e \approx 10^7$–10^{15} cm^{-3}) plasma created by the impact of meteorites with dust-covered boulders [*Goertz and Morfill*, 1983] was sufficient to release electrostatically charged dust grains into the ring system. These charged dust grains may then levitate above the ring plane and form the spokes observed in Saturn's B ring.

Motivated by the dusty boulders in Saturn's rings and dusty spacecraft in the ionosphere, we conducted laboratory experiments to simulate the release of dust from objects in space plasmas and to identify the basic physics that is involved. In this paper we report an experiment pertaining to the short-duration (less than 1 hour) exposure of a dusty body to a plasma.

To our knowledge, this is the first time an experiment has been reported that demonstrates that plasma exposure leads to dust shedding from material bodies. Since this is the first report of this phenomenon, we do not address specialized issues such as longer-duration exposure or the effects of solar radiation, oxygen erosion, and auroral environments, nor have we investigated a wide variety of plasma conditions. These important topics deserve further experimentation in the future.

In section 2 we describe the laboratory apparatus in which these measurements of dust-surface interactions were made. In section 3 we describe the experimental procedure and outline our results, which are discussed in detail in section 4. Section 5 is a summary.

2. APPARATUS

Because of the inherent difficulty of conducting controlled experiments in space to study dust shedding, we have designed a laboratory experiment encompassing the relevant physics. Test bodies are coated with micrometer-sized

[1]Now at Department of Physics, West Virginia University, Morgantown.

[2]Temporarily at Max-Planck Institut für extraterrestrische Physik, Garching, Germany.

Paper number 91JA02801.
0148-0227/92/91JA-02801$05.00

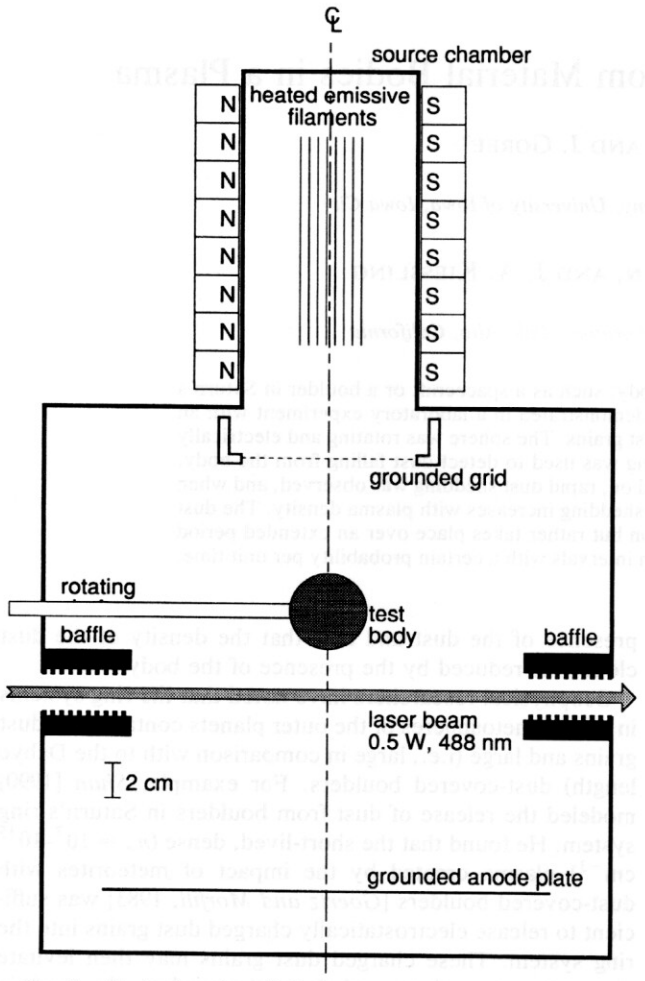

Fig. 1. Scale drawing of the experimental apparatus, viewed from the side. The plasma is created by electron impact ionization of neutral nitrogen gas in the vacuum vessel. Primary electrons are emitted by negatively biased heated filaments. Light scattered from the laser beam indicates the amount of dust falling from the test body.

grains and then placed in a laboratory plasma. To more closely mimic an object in space, these bodies rotate and are electrically floating. The shedding is measured by laser light scattering from the dust as it falls from the body. In the following subsections we discuss the apparatus in detail.

2.1. *Vacuum System*

The experiments were performed in a cylindrical vacuum vessel with an inner diameter of 32.4 cm and a height of 31.6 cm, as shown in Figure 1. The vessel is made of aluminum, and it was anodized black to reduce scattered light. The vessel is evacuated by a turbomolecular pump backed by a rotary-vane pump, attaining base pressures below 8×10^{-5} Pa ($=8 \times 10^{-10}$ atm) after bakeout. Aluminum and nonmagnetic stainless steel hardware have been used to minimize unwanted magnetic field perturbations.

The plasma is created in a source chamber located on the top of the main vessel. A high-transparency stainless steel grid separates the source chamber from the main vessel. For the experiments reported here, this grid was always grounded. A grounded, stainless steel anode plate at the bottom of the main vessel provides a ground reference for the plasma.

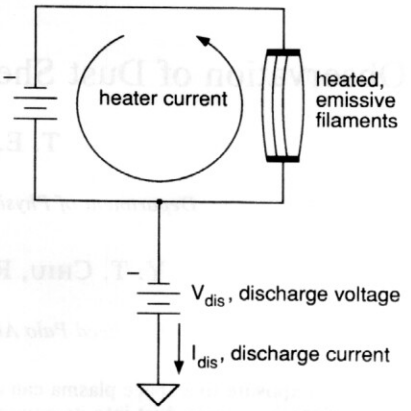

Fig. 2. Schematic of the filament circuit. The filaments are heated by the heater current and are biased negatively at a voltage V_{dis} to emit electrons. When a plasma is formed, a discharge current I_{dis} flows through the biasing power supply. The circuit shown here is completed by the vacuum vessel, which acts as a grounded anode that collects the current emitted by the filaments. When there is no plasma, $I_{dis} = 0$.

2.2. *Plasma*

The plasma is created by a hot filament source, consisting of eight thoriated tungsten filaments, each 12 cm long and 0.007 inch in diameter. These filaments are heated until they become emissive. When the filaments are biased to a negative potential, they emit electrons that can ionize the background gas, creating a plasma. A multidipole magnetic field [*Limpaecher and MacKenzie*, 1973] is used to enhance electron confinement in the source chamber but not in the main chamber. Discharges from this type of source typically have two electron components: a primary component coming directly from the filaments, and a denser, cold plasma component created through impact ionization of the neutral gas by the primary electrons. The current drawn between the filaments and the grounded vacuum vessel is called the discharge current I_{dis}, and it is a simple indicator of the plasma density n_e. These two quantities are proportional, provided that the electron temperature is constant, which it often is.

The filaments are heated and biased independently, as sketched in Figure 2. Consequently there are two ways to control the discharge. First, the discharge current I_{dis} is very sensitive to the temperature of the filaments, which is controlled by the heater power supply. A small increase in the filament temperature causes a large increase in the discharge current. Second, raising the discharge voltage V_{dis} increases the energy of the primary electrons. Because of the low neutral pressures used, this does not greatly increase the discharge current, though the density may be significantly increased. When the discharge voltage falls below the ionization potential of the gas, the discharge is extinguished, and the discharge current becomes zero.

The plasma was characterized using a small cylindrical Langmuir probe with a diameter of 0.010 inch and a length of 3.0 mm. From current-voltage characteristics of the probe [*Chen*, 1965], we determined the plasma potential V_{plasma}, the floating potential V_{float}, the electron density n_e, and the electron temperature T_e. (Before any probe data were taken, the probe's surface was cleaned by drawing a large current from the plasma. It was impossible to take reliable probe

data during the dust shedding experiment because there was no way to clean the probe without making a vigorous discharge, which would have removed all dust from the sphere.) At a discharge voltage of −40 V and a discharge current of 1.0 A, we found $T_e \approx 7.3$ eV and $n_e \approx 10^{13}$ m^{-3}. At this low discharge voltage the electron distribution is somewhat non-Maxwellian, and so we can only roughly estimate the plasma parameters. For a discharge voltage of −60 V and a discharge current of 1.0 A, we found that $V_{\text{plasma}} = 5$ V, $T_e = 4.1$ eV, and $n_e = 1.1 \times 10^{14}$ m^{-3}. Augmenting the discharge voltage increases the plasma density significantly. At lower discharge voltages (i.e., −40 V) an electron beam component is seen in the probe characteristic. This component disappears as the discharge voltage is made more negative. Measurements of the floating potential corroborate this observation; as the discharge voltage becomes more negative, the floating potential becomes less negative.

Some of these plasma parameters in the laboratory experiment differ from those in the Earth's ionosphere and planetary magnetospheres. However, our results remain applicable to many important space physics problems, as we explain here. Our electron temperature approximates that of the auroral regions of the ionosphere. The presence of a fast electron beam component in our experiment is suitable for simulating spacecraft interactions because it is known from simulations [*Machida et al.*, 1988; *Machida and Goertz*, 1986] that water outgassing from a spacecraft leads to plasma velocity-space instabilities that heat the electrons and produce a beam. Our electron density is comparable to that produced by the impact of meteorites with dust-covered boulders. While it is many orders of magnitude higher than the density in the ionosphere, we do investigate in this paper the dependence of dust shedding on plasma density.

2.3. *Test Bodies*

For these experiments, dust was applied to a small aluminum sphere of diameter 4.45 cm. This sphere mimics a dust-covered object in space such as a spacecraft or a rock in Saturn's rings. Experiments also were performed using spheres whose surfaces had been black anodized or wrapped with Mylar tape. Since the results were essentially the same, we present in this paper only the data from the bare aluminum sphere. (The sphere was fabricated by turning it in a lathe, and its surface retained shallow grooves from this process.) Since aluminum naturally forms a surface oxide layer when exposed to the atmosphere, our sphere was covered with a nonuniform dielectric layer. Consequently, it may not always be in very good electrical contact with the plasma. There was no need to actively cool the sphere since it was not heated significantly in the experiment. To simulate the rotation of objects in space, the sphere was mounted on a motor-driven rotating stainless steel shaft. The rotation of the sphere was slightly imperfect, with a jerk due to the design of the bellows-sealed rotary-motion feedthrough and a slight wobble of <2 mm over a rotation.

The sphere was grounded through a large 4-MΩ impedance. Because of this large resistance the sphere drew no significant current from the plasma. In other words, it floated electrically, exactly like an object in space, to the floating potential. This potential (i.e., V_{float}) was recorded by a voltmeter during the experiment.

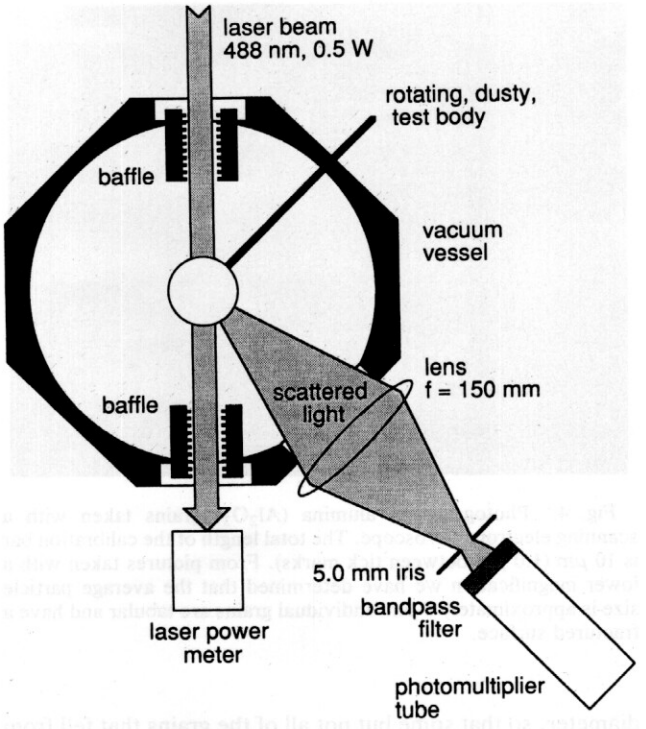

Fig. 3. Top view of the optics used to detect laser light scattered by falling dust grains. Laser light ($\lambda = 488$ nm) scattered at 45° in the forward direction is collected by a 10-cm diameter lens with a focal length of 150 mm. A 5.0-mm diameter circular aperture is placed at the focal point of the lens to define the viewing volume. A 488-nm optical band-pass filter passes the desired scattered laser light while rejecting most of the glow from the white-hot filaments. Finally, the scattered light is converted to a current, called the "scattered light signal," by a photomultiplier tube.

2.4. *Scattered Light Diagnostic*

To record the rate of dust shedding, we employed laser light scattering. An argon ion laser, operating at steady state at a wavelength of 488 nm, was pointed beneath the sphere. Grains falling from the sphere caused Mie scattering that we detected with a photomultiplier tube. The amount of light scattered depends on both the number density and the size distribution of grains. Light scattering from the plasma itself was immeasurably small, and so it did not interfere with our experiment.

Now we explain the geometry of the optical setup. The laser beam entered and exited the vacuum vessel through a pair of quartz windows as shown in Figure 3. A third window was placed 45° from the forward direction to allow the collection of scattered light. This angle was chosen because it takes advantage of the predominantly forward direction of Mie scattering while still allowing a dark background for detecting the scattered light. To reduce stray light, baffles were installed at the input and output windows (see Figure 1). The total power of the laser beam was measured as it passed out of the vacuum vessel.

The optics were aligned to locate the volume from which scattered light was collected at the center of the main vacuum vessel and directly under the test body, as shown in Figures 1 and 3. The laser beam width was 1.8 mm (measured as the full width at half maximum of the transverse power profile), which is much narrower than the sphere

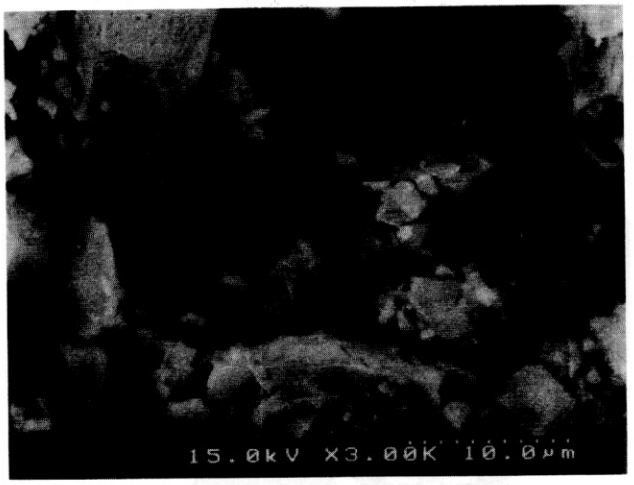

Fig. 4. Photograph of alumina (Al_2O_3) grains taken with a scanning electron microscope. The total length of the calibration bar is 10 μm (1.0 μm between tick marks). From pictures taken with a lower magnification we have determined that the average particle size is approximately 8 μm. Individual grains are tabular and have a fractured surface.

diameter, so that some but not all of the grains that fell from the sphere passed through the beam. Those that did fall through the beam scattered some light, which we detected. The scattered light was collected by a lens, 10 cm in diameter and 150 mm in focal length, placed 45° from the forward direction. It focused the light on a 5.0-mm diameter iris, which defined the scattering volume we detected. The light was then incident on a 488-nm band-pass filter (55% maximum transparency, 3-nm bandwidth), which blocked most of the light from the white-hot filaments. Not all of the white light was blocked, and this contributed to a baseline in our signal that increased with filament temperature. Finally, the filtered light was detected by a photomultiplier tube, and its current was recorded using a meter with a resolution of 0.1 nA. The photomultiplier tube current is hereafter referred to as the "scattered light signal."

2.5. *Dust*

To carry out well-controlled experiments, we applied dust of a known composition and size to the sphere. In selecting the type of dust, our requirements were a dielectric composition, with particle sizes ranging from 1 to 10 μm. In addition, we wanted the dust to be free-flowing when in bulk (i.e., it should not clump when handled), so that particles could be released individually from the surface of our sphere. To characterize their size and morphology, candidate dust specimens were imaged with a scanning electron microscope. This was a valuable procedure because it revealed that some dust samples purchased from scientific suppliers are composed of grains that are much larger than advertised. On the basis of this discovery, we can offer the advice that to carry out a controlled experiment with dusty plasmas, one should first use an electron microscope to characterize the dust.

We chose to use Alcoa tabular (i.e., "tablet" shaped) alumina (Al_2O_3) for these experiments. This is a free-flowing white powder with a characteristic grain size (width) of about 8 μm, as shown in Figure 4. The smallest grains are approximately $\frac{1}{4}$ μm in size. Individual grains have a flaked surface. The density of alumina is 3.9 g/cm^3, so that an 8-μm diameter sphere would have a mass of approximately 1.1 ng. The average mass of a grain, determined from a rough size distribution taken from an electron micrograph, is $\approx$0.3 ng. Finally, we note that the dielectric constant of alumina [*Weast*, 1978] ranges from 4.5 to 8.4.

3. EXPERIMENT

The purpose of the experiment was to determine whether a plasma would influence dust shedding form a dusty body. As such, the experiment consisted of two steps: applying dust to the test body and detecting the dust shedding in a plasma.

3.1. *Preparation of Test Bodies*

Test bodies were prepared in air before insertion in the vacuum vessel. Before dust was applied, the surface of the sphere was cleaned with isopropyl alcohol. Alumina dust was applied to the test spheres electrostatistically. The sphere was biased to a high potential using a Van de Graaff generator and then moved over a dust-covered glass plate. Electrostatic attraction picked dust up from the plate and deposited it on the sphere. This procedure allowed us to coat the surface fairly uniformly with a large quantity of dust in a reproducible manner. After applying the dust, we grounded the sphere so that it no longer had a charge. The dust remained attached to the body by adhesion.

By weighing the dust scraped off an untreated aluminum sphere, we found that 80 $\pm$ 10 mg of alumina dust had been applied. We estimate that 80 mg of dust contains roughly 2×10^8 individual grains.

After the vacuum vessel was filled with argon to atmospheric pressure, the test sphere was inserted, and the vessel was sealed. A valve to the pumps was then opened to begin the evacuation. During the first minute of pumping, the pressure decreased rapidly, and a small amount of dust shedding was observed, presumably from the wind. This is interesting for understanding dust shedding during and after a rocket flight into space. A payload undergoes both depressurization and mechanical vibration, and one might ask whether this can loosen the dust from the payload before it is exposed to a space plasma. To compare the effects of depressurization and mechanical vibration in a simple, nonquantitative way, we tapped on the shaft supporting the test sphere to shake it a little. We found that mechanical vibrations can release much more dust than depressurization. From this simple test we concluded that depressurization is not a significant source of dust release. Dust shedding is caused more profoundly by mechanical vibration and, more importantly, by exposure to a plasma, as we demonstrate next.

3.2. *Results of Plasma-Dust Experiments*

For this experiment we measured the dust shedding under a variety of plasma conditions. Time histories of the discharge current, discharge voltage, scattered light signal (i.e., the photomultiplier tube signal), and floating potential are shown in Figures 5–7. These quantities were sampled approximately twice per second. The experiments was performed with nitrogen at a pressure of 0.056 Pa, and to

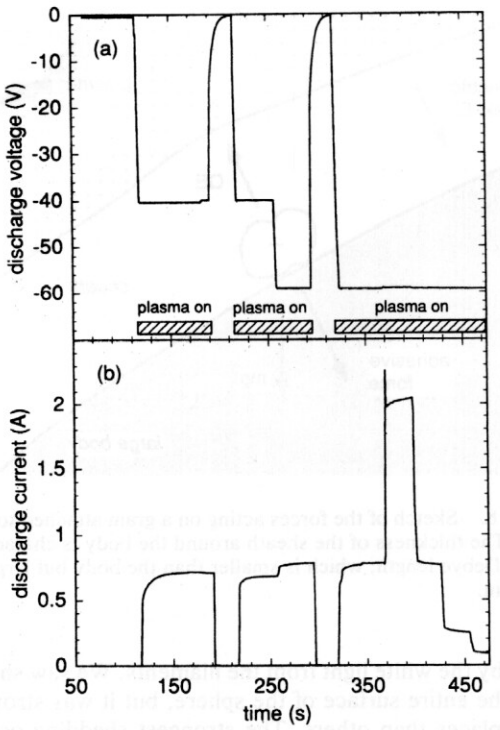

Fig. 5. Time histories of (*a*) discharge voltage V_{dis} and (*b*) discharge current I_{dis}. There is no plasma when $I_{dis} = 0$. The plasma was deliberately switched off and on to observe the plasma's effect on dust shedding. During the plasma-on intervals we operated at several different discharge voltages and currents.

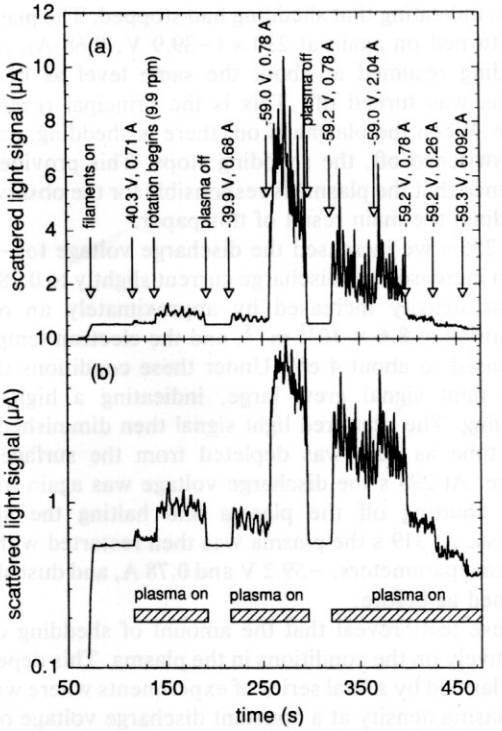

Fig. 6. Time histories of the scattered light signal for dust shedding from an untreated aluminum sphere coated with ≈80 mg of alumina dust. The data are plotted (*a*) on linear axes and (*b*) on semilogarithmic axes. In Figure 6*a*, times of particular interest have been marked. When the plasma is on, the average discharge voltage and current are given. The baseline is due to light from the hot filaments, and it varies with the filament temperature. Dust shedding is indicated by spikes above the baseline. Dust shedding is seen only when the plasma is on, indicating that shedding is caused by the interaction between dust grains, the sphere, and the plasma.

maintain the desired pressure there was a continuous flow of nitrogen gas through the vessel. The laser power was 0.37 W.

First, the filaments were turned on without a plasma. Then a plasma was formed, and we switched it on and off several times. In examining Figure 6, one should look for spikes in the scattered light signal; these indicate scattering from dust grains. Let us review now the detailed time history of the experiment.

At 66 s we began heating the filaments. At this time the signal increased to a steady baseline level, seen in Figure 6, due to light from the white-hot filaments. This baseline comes from the small transmission of the white filament glow through the optical filter and should not be confused with dust shedding. The filaments then remained on for the rest of the experiment. Note that since the discharge voltage is zero, there is no plasma, as indicated by the zero discharge current.

A plasma was formed at 116 s by turning the discharge voltage on to −40.3 V. This resulted in a discharge current of 0.71 A. Under these conditions the electron temperature is about 7 eV, and the density is around 7×10^{12} m^{-3}. A scattered light signal is evident above the baseline signal from the filaments, indicating weak shedding. In this plasma the floating potential of the sphere was −17 V, as shown in Figure 7.

At 140 s the sphere was started rotating at 9.9 rpm. There is a small increase in the scattered light signal as dustier areas on its surface are brought under the plasma source. In addition, the scattered light and the floating potential are modulated at the rotation frequency, which is apparently due to wobble of the sphere on its shaft and not due to dust shedding.

At 190 s we turned the plasma off by turning the discharge voltage to zero. The light signal returned to its baseline

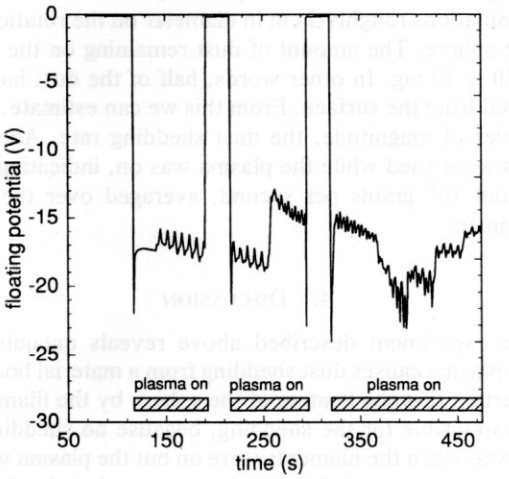

Fig. 7. Time history of the floating potential V_{float} of the test body. The floating potential is negative and is modulated at the rotation frequency. As the rate of shedding decreases, the floating potential becomes more negative.

value, indicating that shedding had stopped. The plasma was then turned on again at 230 s (−39.9 V, 0.68 A), and dust shedding resumed at about the same level as before the plasma was turned off. This is the principal result of the paper. When the plasma is on, there is shedding, and when it is switched off, the shedding stops. This provides direct evidence that the plasma is responsible for the observed dust shedding, the main result of this paper.

At 256 s we increased the discharge voltage to −59.0 V, which increased the discharge current slightly to 0.78 A. The plasma density increased by approximately an order of magnitude to 8.6×10^{13} m^{-3}, and the electron temperature decreased to about 4 eV. Under these conditions the scattered light signal grew large, indicating a high rate of shedding. The scattered light signal then diminished slowly with time as dust was depleted from the surface of the sphere. At 295 s the discharge voltage was again turned to zero, shutting off the plasma and halting the shedding process. At 319 s the plasma was then restarted with nearly the same parameters, −59.2 V and 0.78 A, and dust shedding resumed as before.

These tests reveal that the amount of shedding depends sensitively on the conditions in the plasma. This dependence was clarified by a final series of experiments where we varied the plasma density at a constant discharge voltage of −59.2 V. (Recall that for a constant V_{dis} the plasma density is proportional to the discharge current.) To do this we changed the heater current, which controls the temperature of the filaments, and consequently the discharge current. (This also shifts the baseline of the light signal by changing the brightness of the filaments.)

This series of plasma densities began at 368 s, when the discharge current was increased to 2.0 A. The rate of shedding increased with the plasma density but then resumed its slow decline. We then lowered the discharge current several times, to 0.78, 0.26, and 0.092 A at times 398, 466, and 416 s, respectively. Each time the shedding rate diminished, and at the lowest discharge current it became almost undetectable. Consequently, we conclude that dust shedding is stronger in a denser plasma.

After the experiment was completed, the sphere was removed from the vacuum vessel and examined. A uniform coating of dust remained everywhere, with additional small accumulations roughly 2 cm in diameter on the rotation axes of the sphere. The amount of dust remaining on the sphere was 50 ± 10 mg. In other words, half of the dust had been scoured from the surface. From this we can estimate, within an order of magnitude, the dust shedding rate. About 10^8 grains were shed while the plasma was on, indicating a rate of about 10^6 grains per second, averaged over the entire experiment.

4. DISCUSSION

The experiment described above reveals unequivocally that a plasma causes dust shedding from a material body. We are certain that the heating of the sphere by the filaments is not responsible for the shedding, because no shedding was observed when the filaments were on but the plasma was off.

What is not revealed by the laser scattering signal shown in Figure 6 is where on the sphere the dust comes from. This requires imaging, which we have also carried out by visual and videocamera observations in which the dust was illuminated by the white light from the filaments. We saw shedding from the entire surface of the sphere, but it was stronger in some places than others. The strongest shedding occurred on the top of the sphere, which is exposed directly to the filaments. This is likely due to the flux of primary electrons from the filaments impinging on the top of the sphere. The top of the sphere did not become depleted rapidly because the rotation of the sphere served constantly to carry dustier areas under the filaments.

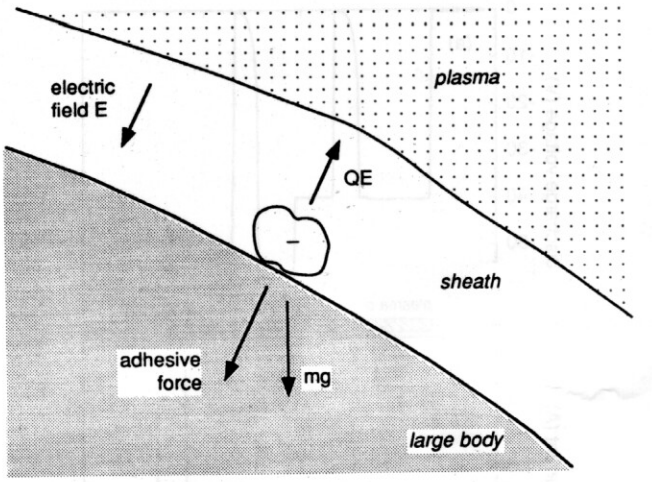

Fig. 8. Sketch of the forces acting on a grain attached to a large body. The thickness of the sheath around the body is characterized by the Debye length, which is smaller than the body but larger than the grain.

4.1. *Dust Shedding*

4.1.1. *The various forces acting on a grain.* Having established that plasma-dust interactions are responsible for the shedding, we now attempt to identify the basic physics. We first identify the forces acting on the grains: adhesive, electric, and gravity, as sketched in Figure 8. In our laboratory experiment the centrifugal force due to rotation was negligible because it was 4 orders of magnitude weaker than gravity.

Chemical adhesive forces bind the dust grains in varying degrees to the surface of the body. These forces are at work in everyday surroundings, holding dust onto every surface. The adhesive force surely varies with the material of both the surface and the grains, as well as the size of grains. There is no doubt that it can be strong enough to overcome the pull of gravity, as one can easily demonstrate by turning upside down any object at hand and observing that most of the dust remains attached. This might seem too obvious to mention, except that it helps in comparing the strength of the forces in our experiment. In preparing the dusty coating on our sphere we turned the sphere upside down many times, and so we know that for the dust that remained on the sphere, the adhesive force was stronger than gravity alone. To be shed, an additional force is needed. When immersed in a plasma, an electric force arises, and it plus the gravitational force must exceed the adhesive force if dust is to be released. Once the grain has been shed from the surface, there is no longer any adhesive force, while the other forces continue to act to it.

The electric force QE results from the charge Q on the

grain and the electric field E in the sheath of the body. First, let us consider the electric field E. In a plasma the sphere floats to a negative potential with respect to the plasma, and a plasma sheath surrounds it. (This assumes that secondary electron emission is negligible; otherwise, it could float to a positive potential [*Goertz*, 1989].) The plasma sheath has a nonuniform electric field that is strongest at the sphere's surface. The typical scale length for the sheath is the Debye length λ_D (at the sheath-plasma boundary), and the typical potential drop is the floating potential referenced to the plasma potential, $\phi = V_{\text{float}} - V_{\text{plasma}}$. Recall that this is a negative potential, and it should be compared to kT_e/e. If the electrons in the plasma are Maxwellian, ϕ will be of the order of $3kT_e/e$, while if an electron beam is present, ϕ will be augmented to a value that can be as high as the beam energy. The electric field in the sheath of the floating body is of the order of ϕ/λ_D. More exactly, E at the surface is given by [*Chen*, 1974]

$$E = \frac{kT_e/e}{\lambda_D} 2^{1/2}\left[\left(1 - \frac{2e\phi}{kT_e}\right)^{1/2} + \exp\left(\frac{e\phi}{kT_e}\right) - 2\right]^{1/2}, \quad (1)$$

which is derived from planar sheath theory by approximating the surface of the dusty sphere as a plane and assuming that ions flow into the sheath edge at the ion acoustic velocity, which is a safe assumption for a Maxwellian plasma [*Chen*, 1974].

In our experiment the electric field computed from (1) is $E = 41$ V/cm for the following plasma parameters: $T_e = 4$ eV, $\phi = -20$ V, $n_e = 8.6 \times 10^{13}$ m^{-3}, and $\lambda_D = 1.6$ mm, which are for a discharge operated at $V_{\text{dis}} = -60$ V and $I_{\text{dis}} = 0.78$ A. The direction of the electric field E will point toward the sphere. This is important because it means that the direction of the electric force will be away from the surface, thereby promoting shedding of the dust, provided the grains are negatively charged.

The grain acquires a charge Q while it rests on the sphere's surface. This charge arises from the impinging fluxes of ions and electrons [*Goertz*, 1989]. It is related to V_{grain}, the potential of the grain with respect to the local plasma potential, by the relation $Q = CV_{\text{grain}}$, where C is a capacitance. If the particle is spherical and it acts like a capacitor of its own (this despite its being attached to a larger sphere, a matter we discuss later), then

$$C = 4\pi\varepsilon_0 a, \quad (2)$$

where a is the radius of the grain. The potential V_{grain} should typically be close to the potential V_{float} of the conducting sphere, which is independent of the grain size, and so the charge Q and the electric force QE are both proportional to a. The adhesive force is presumably proportional to surface area a^2, while the mass and thus the force of gravity scale with the volume of the grain, a^3. These three scaling laws suggest that gravity will tend to pull the largest grains from the surface while the electric force will first remove the smallest grains.

4.1.2. *Estimate of charge on a grain attached to the body.* The charge Q on a grain may be roughly estimated by comparing the electrical force to the gravitational force. We know from our visual observations that dust was often shed from the top of the sphere. This indicated that the electric force QE was greater than gravity.

$$|Q|E > mg, \quad (3)$$

where m is the mass of a grain. This upward levitation allows us to estimate a lower limit on Q. For the case of an 8-μm diameter spherical grain we find

$$|Q| > 15{,}000e \quad (4)$$

where e is the elementary charge. If we assume that the capacitance C is given by (2), then the calculated potential ($V_{\text{grain}} = Q/C$) of an 8-μm grain is approximately -5 V. This value is in order of magnitude agreement with the floating potential $\phi = -20$ V on the aluminum sphere. As the mass of a grain is proportional to the cube of its radius, the lower limit of Q (computed in this way from our experimental results) decreases rapidly with grain size.

This result reveals some of the physics of how the grain charges while it is attached to the sphere. The question that it answers is whether the grain merely acts as part of the surface area of the entire sphere, with the charge uniformly distributed over the sphere. If that were so, then Q would be much smaller, and indeed it would usually be either zero or only one electron charge. This was assumed to be the case by *Shan* [1990] in a numerical simulation of the dust shedding from boulders in the rings of Saturn, a process that has been claimed to explain the spokes in Saturn's rings [*Goertz and Morfill*, 1983; *Goertz*, 1989]. Such a low charge would not be enough to overcome adhesion and result in shedding, and as a result Shan had to assume that any dust that was released from Saturn's rings came from the void between boulders, where grains are gravitationally confined, with less binding energy than the adhesion of grains on the boulders themselves.

In the absence of any experimental test, the idea that the grain merely acts as part of the surface might seem reasonable. However, this assumption is not verified by our experiment, at least not for our parameters: plasma exposure durations of many seconds and plasma densities of typically 10^{14} m^{-3}.

Our experiment demonstrates that the grain acquires a much higher charge, typically thousands of electron charges, while it is attached to the body. This large charge is comparable to the charge the grain would have in the plasma after it is detached from the sphere. It shows that the grain acts like a little capacitor of its own and not like part of the big sphere's capacitance. This result presumably owes to the dielectric material of the dust grains.

4.1.3. *Dependence on plasma parameters.* How the shedding depends on the plasma density and floating potential is revealed in the scattered light data. The shedding is stronger in denser plasmas, as seen in the plasma density scan in the interval $319 < t < 466$ s.

Exactly how the plasma density determines the shedding rate is unknown. Any explanation must certainly center on the electric force QE, which has to overcome the adhesive force for shedding to take place. We offer two qualitative explanations; one or both of them may explain the density dependence. First, the surface electric field E increases with the square root of n_e, as predicted by (1), so a higher density yields a larger electric force. The profound effect of a larger E may be revealed by comparing two discharges before and after 256 s. According to (1), the discharge at -59 V has an electric field that is fourfold larger, which is consistent with

the experimental result that it has a much higher shedding rate. Second, a higher density corresponds to a higher number flux of electrons and ions to the surface and to each grain. If the microscopic process that determines the charge Q of a grain depends on the finite time interval between the arrival of individual electrons and ions on the grain surface, then Q and the electric force QE would depend on the plasma density.

4.1.4. *Grain shedding at random intervals.* We may also infer that the probability per unit time (of a grain being shed) remains roughly constant under constant plasma conditions. We arrive at this conclusion from noting that the scattered light signal in Figure 6*b* decays exponentially for constant plasma conditions. To identify the exponential decay, look for a linear decrease in Figure 6*b* with semilogarithmic axes. Data taken using the spheres coated with black anodizing and Mylar tape also revealed the same exponential decay. Grains are shed from the surface at a rate that is proportional to the amount remaining.

From this we conclude that the shedding process occurs with individual grains jumping off at random intervals. The probability per unit time of one grain jumping off remains roughly constant provided that the plasma conditions do not change. This result is interesting, because one might have expected instead that the grains would be shed in a single burst the moment the plasma is first turned on. The random nature of the dust shedding indicates that the mechanism of releasing the grains from the surface depends on some quantity that varies statistically with time. The physics of this random process is unknown.

4.2. *Floating Potential*

From the time history of the floating potential shown in Figure 7 we may glean further information about the physics relevant to the shedding process. As with the scattered light signal, the floating potential is modulated by the 9.9-rpm rotation of the sphere. Some modulation in V_{float} is observed even for a clean aluminum sphere and may be due to a nonuniform oxide layer on the surface of the sphere. Interestingly, for constant plasma conditions, whenever the strength of shedding decreases, the floating potential becomes more negative. This is true for both the rotational modulation and the slow decay in the rate of shedding. Two possible explanation for this phenomenon are consistent with the data.

First, negatively charged dust grains leaving the sphere constitute a negative current from the sphere or, conversely, a positive current to the sphere. (Recall that a grain may carry many thousands of electron charges.) This current, together with the electron and ion currents, determines the floating potential of the sphere. Since the current carried by the dust is like an ion current on the sphere, the floating potential during the dust shedding will be less negative than without dust shedding. As the rate of shedding decreases, the floating potential becomes more negative since the negative charge carried away from the sphere is reduced.

Second, grains in the plasma are negatively charged (again assuming surface electron emission processes are negligible). If a grain collects additional electrons in the plasma (i.e., more than it carried when it first left the sphere's surface), then the electron density in the plasma will be reduced in relation to the ion density. When the dust density in the plasma is large, the electron density will be small, and V_{float} will be less negative. As the rate of shedding decreases, the dust density in the plasma also decreases, increasing the electron density and causing the floating potential to become more negative.

5. SUMMARY

We find that dust is rapidly removed from an electrically floating test body immersed in a plasma. Since the shedding is observed only with the plasma on, we conclude that the interaction between the dust grains on the body and the plasma is responsible for the dust shedding. Individual grains are shed at random intervals, where the probability per unit time that a grain jumps off the surface increases with plasma density. Rotation of the body enhances the shedding rate by bringing fresh dusty surfaces so that they face the source of fast electrons in the plasma. These results should be useful in showing how dust-spacecraft interactions should be taken into account in designing future missions and in understanding the production of dusty plasmas in planetary ring systems.

Acknowledgments. This paper is dedicated to the memory of our friends and colleagues who died at The University of Iowa on November 1, 1991: Christoph Goertz, Dwight Nicholson, Lin-hua Shan, and Robert Smith. We gratefully acknowledge discussions of this paper with Christoph Goertz and Lin-hua Shan. This work was supported by Lockheed Missiles and Space Company, under contract 605352-L from The Applied Physics Laboratory of the Johns Hopkins University.

The Editor thanks Associate Editor J. U. Kozyra for handling the review process on this paper and T. P. Armstrong and E. Whipple for their assistance in evaluating this paper.

REFERENCES

Chen, F. F., Electric probes, in *Plasma Diagnostic Techniques*, edited by R. H. Huddlestone and S. L. Leonard, pp. 113–200, Academic, San Diego, Calif., 1965.

Chen, F. F., *Introduction to Plasma Physics*, p. 246, Plenum, New York, 1974.

Goertz, C. K., Dusty plasmas in the solar system, *Rev. Geophys.*, *27*, 271, 1989.

Goertz, C. K., and G. Morfill, A model for the formation of spokes in Saturn's rings, *Icarus*, *53*, 219, 1983.

Limpaecher, R., and K. R. MacKenzie, Magnetic multipole containment of large uniform collisionless quiescent plasmas, *Rev. Sci. Instrum.*, *44*, 726, 1973.

Machida, S., and C. K. Goertz, A simulation study of the critical ionization velocity process, *J. Geophys. Res.*, *91*, 11,965, 1986.

Machida, S., C. K. Goertz, and G. Lu, Simulation study of the critical ionization velocity process, *J. Geomagn. Geoelectr.*, *40*, 1205, 1988.

Murphy, D. L., and Y. T. Chiu, Dusty plasmas in the vicinity of a large dielectric object in space, *J. Geophys. Res.*, *96*, 11,291, 1991.

Shan, L., Electromagnetic effects in Saturn's B ring, Ph.D. thesis, Univ. of Iowa, Iowa City, 1990.

Weast, R. C. (Ed.), *CRC Handbook of Chemistry and Physics*, p. E-60, CRC Press, Boca Raton, Fla., 1978.

(Received July 21, 1991;
revised October 21, 1991;
accepted October 22, 1991.)